LANGMUIR Article
Cite This: Langmuir 2018, 34, 10782−10792
pubs.acs.org/Langmuir

Multistep Interactions between Ibuprofen and Lipid Membranes

Simou Sun,[†] Anne M. Sendecki,[†] Saranya Pullanchery,[†] Da Huang,[†] Tinglu Yang,[†] and Paul S. Cremer*[,†,‡]

[†]Department of Chemistry, Penn State University, University Park, State College, Pennsylvania 16802, United States
[‡]Department of Biochemistry and Molecular Biology, Penn State University, State College, Pennsylvania 16802, United States

Supporting Information

ABSTRACT: Ibuprofen (IBU) interacts with phosphatidylcholine membranes in three distinct steps as a function of concentration. In a first step (<10 μM), IBU electrostatically adsorbs to the lipid headgroups and gradually decreases the interfacial potential. This first step helps to facilitate the second step (10−300 μM), in which hydrophobic insertion of the drug occurs. The second step disrupts the packing of the lipid acyl chains and expands the area per lipid. In a final step, above 300 μM IBU, the lipid membrane begins to solubilize, resulting in a detergent-like effect. The results described herein were obtained by a combination of fluorescence binding assays, vibrational sum frequency spectroscopy, and Langmuir monolayer compression experiments. By introducing trimethylammonium-propane, phosphatidylglycerol, and phosphatidylethanolamine lipids as well as cholesterol, we demonstrated that both the chemistry of the lipid headgroups and the packing of lipid acyl chains can substantially influence the interactions between IBU and the membranes. Moreover, different membrane chemistries can alter particular steps in the binding interaction.

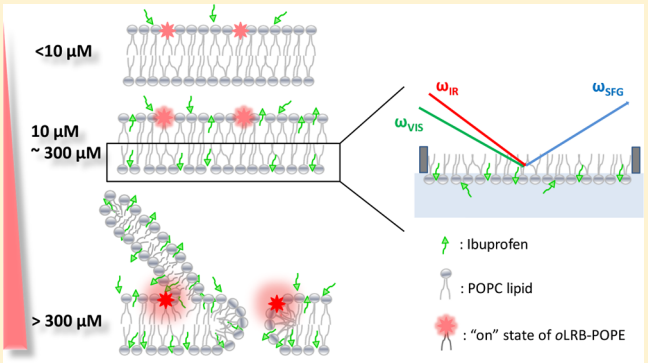

Small soluble drug molecules can partition from the aqueous phase into lipid bilayers and alter their physical properties. This, in turn, can influence the interactions between drug molecules and their target membrane-bound proteins.[1−3] Investigations into the location of small molecule drugs in lipid membranes and the molecular level details of these interactions can help to elucidate drug-transport properties, circulation lifetimes, potential side effects, as well as provide valuable insights into drug development and modification.[1,4,5]

Ibuprofen (IBU) is a widely consumed small molecule drug, belonging to the nonsteroidal anti-inflammatory drug family. The primary effect of IBU is related to the nonselective inhibition of cyclooxygenase (COX) enzymes, which are membrane-bound proteins. The binding of IBU to COXs prevents prostaglandin synthesis, leading to its anti-inflammatory and pain killing properties.[6] Studies have shown that IBU can also suppress the intracellular production of reactive oxygen species and the oxidative modification of low-density lipoproteins.[7] Moreover, IBU has been a recommended part of the treatment for a wide variety of diseases, including cancer and Alzheimer's.[8,9] There has been evidence that IBU favorably interacts with lipid membranes. For example, it was reported that IBU can lead to bilayer thinning, a decrease in the membrane bending modulus, enhanced membrane permeability, and an increase in lipid headgroup hydration.[10−13] Interestingly, when the IBU concentration was in the μM range, the drug was reported to stabilize phosphatidylcholine (PC) lipid monolayers.[14,15] However, when the drug concentration reached the mM range, the monolayer was disrupted. Thus, IBU was proposed to have COX-independent effects by interacting with cell membranes.[16]

Although previous literature has provided qualitative insights into IBU binding at lipid membrane interfaces,[10−17] a molecular level picture of the interactions between this small molecule and the lipid membrane is still lacking. Specifically, the location and behaviors of IBU within the bilayer have been controversial.[10,15,18] Moreover, there have been few systematic and mechanistic studies on IBU−lipid membrane interactions as a function of concentration, especially in the low μM range. This is because of the dearth of sufficiently sensitive techniques to probe small molecules at biointerfaces without attaching a fluorescent label to the target molecules.

The motivation behind the present study is 3-fold: (1) to explore the binding behavior of IBU with lipid membranes over a wide concentration range, from sub μM to 15 mM; (2) to discern the location of IBU molecules within lipid bilayers; (3) to determine how the addition of different lipids affects IBU binding. This last point is of particular importance as previous work mainly focused on IBU−phosphatidylcholine interactions.[10−17]

Received: June 9, 2018
Revised: August 3, 2018
Published: August 27, 2018

DOI: 10.1021/acs.langmuir.8b01878
Langmuir 2018, 34, 10782−10792

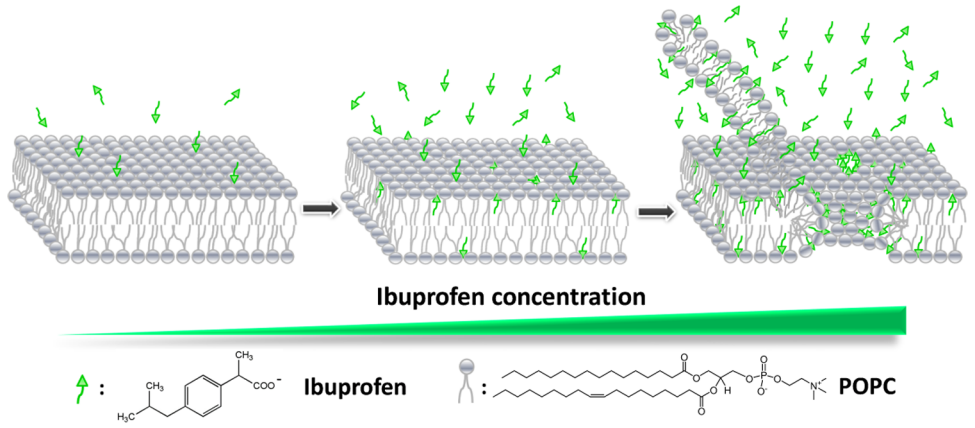

Figure 1. Schematic illustration of the three-step interaction mode between IBU and POPC bilayers.

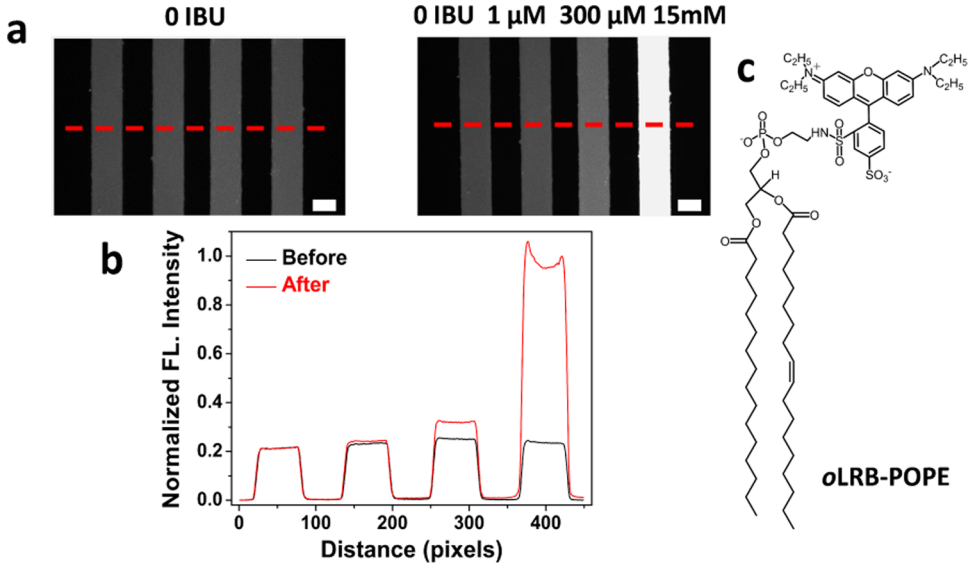

Figure 2. (a) Left: fluorescence micrograph of a four-microchannel device coated with POPC bilayers before the introduction of IBU. The experiments were conducted in 50 mM phosphate buffer at pH 6.9 ± 0.1. Right: different concentrations of IBU solutions were introduced into each channel, from left to right: 0 μM, 1 μM, 300 μM, and 15 mM. The red dashed lines represent the regions over which the linescans were obtained. Scale bar: 0.1 mm. (b) Fluorescence intensity profile of the corresponding linescans before and after the introduction of IBU solutions. (c) Molecular structure of *o*LRB−POPE with the fluorophore in the "on" state. The "off" state is depicted in Figure S1.

To investigate the interactions between IBU and lipid membranes, we used a fluorescence-based assay in which supported lipid bilayers (SLBs) were coated inside a microfluidic platform.[19−23] The pH sensitive lipid−dye conjugate, *ortho*-lissamine rhodamine B (*o*LRB)−1-palmitoyl-2-oleoyl-*sn*-glycero-3-phosphoethanolamine (POPE), was employed as a probe.[22,23] This molecule showed increased fluorescence intensity at more negative interfacial potentials. Since IBU is negatively charged near physiological pH, it gave rise to increased fluorescence signals upon binding to the membrane interface in which the probe was embedded (for details, see the Materials and Methods part of the Supporting Information). This sensing strategy obviated the need to directly tag the analyte with a large, hydrophobic dye, while retaining the high sensitivity of fluorescence assays. It was found that IBU interacted with PC lipids in three consecutive steps with increasing concentration (Figure 1). The first step was dominated by electrostatic adsorption, which saturated at an IBU concentration of 10 μM. In the second step, IBU inserted into the lipid bilayers through hydrophobic interactions. Significantly, the first step could help facilitate the second one because it increased the fluidity of the lipid bilayer and lowered its area stretch modulus,[24] which made hydrophobic insertion possible. This effect acted to expand the membrane area per lipid and saturated at 300 μM. Further increasing the IBU concentration into the mM concentration range caused membrane solubilization, the formation of tubules as well as hole formation in the SLBs. Complementary Langmuir monolayer isothermal compression experiments and vibrational sum frequency spectroscopy (VSFS) measurements on lipid monolayers were conducted to provide molecular level insights into the binding profiles. In addition, positively charged 1,2-dioleoyl-3-trimethylammonium-propane (DOTAP) and negatively charged 1-palmitoyl-2-oleoyl-*sn*-glycero-3-phospho-(1′-*rac*-glycerol) (POPG) were introduced into the membrane to probe electrostatic interactions. The effects of cholesterol and POPE were also systematically studied, and both had pronounced effects on IBU−membrane interactions.

DOI: 10.1021/acs.langmuir.8b01878
Langmuir 2018, 34, 10782−10792

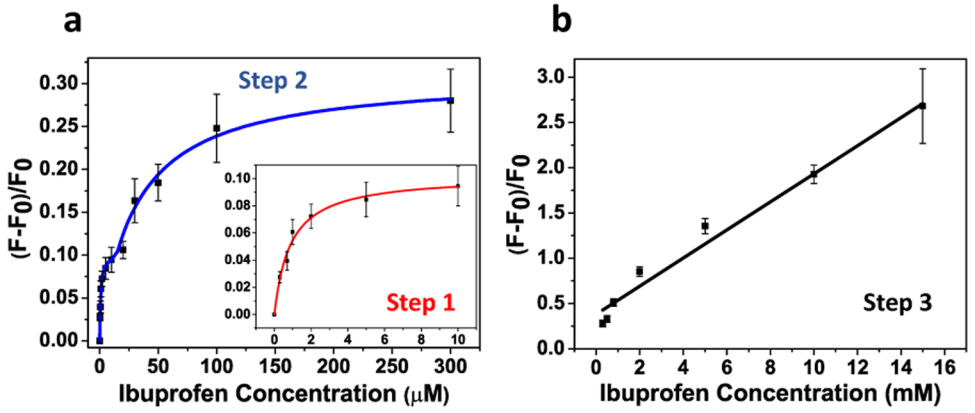

Figure 3. (a) Binding profile of POPC bilayers with IBU in the concentration range from 0 to 300 μM. The black squares are the data points. The blue curve is a combination of two consecutive Langmuir binding isotherms. The first step from 0 to 10 μM is shown in expanded form in the inset and the second step is from 10 to 300 μM. (b) Fluorescence signal change with high concentrations of IBU (300 μM to 15 mM). The data points in this range can be fit to a straight line.

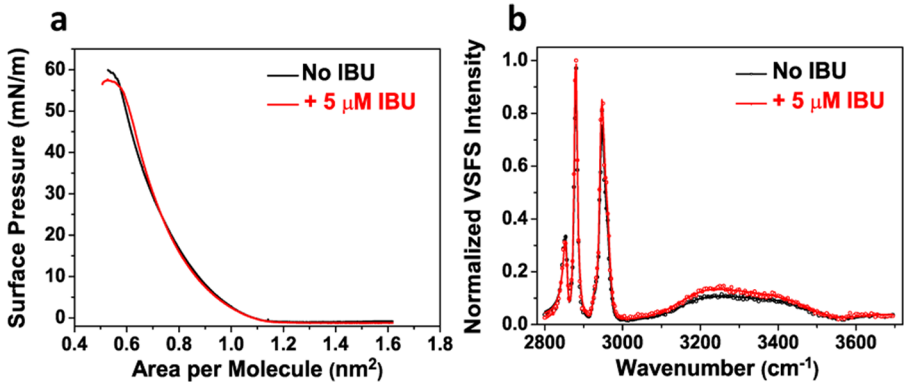

Figure 4. (a) Surface pressure−area isotherms of a DLPC monolayer before (black curve) and after (red curve) the introduction of 5 μM IBU into the aqueous subphase. (b) VSFS spectra of a DLPC monolayer in the CH and OH stretch regions at 30 mN/m before (black curve) and after (red curve) the addition of 5 μM IBU into the aqueous subphase. The dots represent VSFS data points, and the solid lines are fits to the data.

RESULTS

IBU Interacts with POPC Bilayers in Three Consecutive Steps. PC lipids account for >50 mol % of the phospholipids in most eukaryotic cell membranes.[25] As such, SLBs containing 99.5 mol % 1-palmitoyl-2-oleoyl-*sn*-glycero-3-phosphocholine (POPC) with 0.5 mol % *o*LRB−POPE (Figure 2c) were utilized as a starting point to study IBU−lipid bilayer interactions. Bilayers were formed inside poly(dimethylsiloxane)/glass channels by spontaneous vesicle rupture.[26] Buffer was then flowed through the channels until the fluorescence stabilized. The experiments were conducted at room temperature (21 ± 1 °C). Next, IBU solutions at concentrations from 0 μM to 15 mM were introduced into the channels. Increasing fluorescence signal was observed as the IBU concentration was increased (Figure 2).

Fluorescence intensity changes before and after IBU introduction could be plotted as a function of drug concentration to obtain a binding profile (Figure 3). Specifically, the *y*-axis plots the change in fluorescence intensity after introducing IBU compared to pure buffer solution ($(F - F_0)/F_0$). F and F_0 correspond to the fluorescence intensity from the bilayer at a particular concentration of the drug solution and with pure buffer. Curiously, the binding profile had a complex shape. The data are presented in two separate concentration ranges in Figure 3 (0−300 μM and 300 μM to 15 mM). In the lower concentration range, we observed two consecutive binding steps (Figure 3a) with the first step from 0 to 10 μM (inset) and the second step from 10 to 300 μM. The binding profiles for the individual steps fit well to a Langmuir isotherm

$$\frac{F - F_0}{F_0} = \frac{F_{max} - F_0}{F_0} \times \left(\frac{[IBU]}{K_D + [IBU]} \right)$$

where [IBU] is the bulk IBU concentration and F_{max} is the fluorescence intensity of the bilayer with the highest concentration of IBU solution. The extracted K_D values are: K_{D1} = 0.88 ± 0.28 μM and K_{D2} = 30 ± 8 μM. A value corresponding to the first step has not been reported previously, but K_{D2} corresponds well to the value found by UV−Vis sum frequency generation spectroscopic experiments for IBU binding to 1,2-dioleoyl-*sn*-glycero-3-phosphocholine (DOPC) SLBs.[27] Moreover, the fluorescence signal increased in a linear fashion in the high IBU concentration range (Figure 3b). This appears to be indicative of an unsaturable interaction.

Step 1: Electrostatic Interactions between IBU and Lipid Headgroups. We applied two interfacial techniques to investigate the mechanism associated with the first binding step: Langmuir monolayer compression experiments and VSFS measurements. Both measurements employed lipid monolayers at the air−water interface and the experiments were conducted with 1,2-dilauroyl-*sn*-glycero-3-phosphocholine (DLPC),

DOI: 10.1021/acs.langmuir.8b01878
Langmuir 2018, 34, 10782−10792

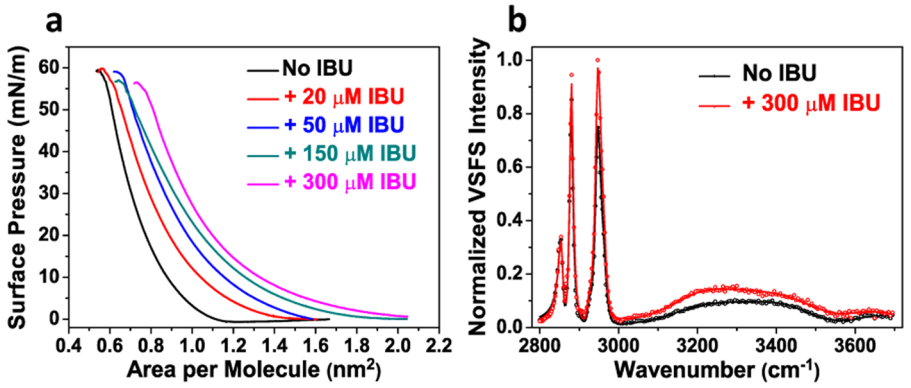

Figure 5. (a) Surface pressure−area isotherms for DLPC monolayers before (black curve) and after the addition of different concentrations of IBU into the aqueous subphase. (b) VSFS spectra of a DLPC monolayer in the CH and OH stretch regions at 30 mN/m before (black curve) and after (red curve) the addition of 300 μM IBU into the aqueous subphase. The dots represent VSFS data points, and the solid lines are fits to the data.

which is in the fluid phase at room temperature, yet has fully saturated tails to avoid lipid oxidation.[28]

Figure 4a shows results from surface pressure−area isotherm measurements. As can be seen, no changes were observed in the presence of 5 μM IBU in the aqueous subphase compared to its absence. This result suggests that the binding of low concentrations of IBU does not alter the packing of the PC monolayer. As such, the drug molecule should mainly interact with the headgroup region. Figure 4b shows VSFS spectra of DLPC monolayers with and without 5 μM IBU. This experiment was performed at 30 mN/m, which is the equivalent lateral pressure of a lipid bilayer.[29] The sharp peaks between 2800 and 3000 cm^{-1} can be assigned to CH stretches (for detailed assignments, see Table S1).[30,31] The broad spectral feature from 3000 to 3550 cm^{-1} can be attributed to interfacial OH stretches aligned by the zwitterionic PC headgroups.[32] With 5 μM IBU in the subphase, no noticeable change was observed in the CH stretch region compared to its absence. This result supports the conclusion from the monolayer compression experiments in Figure 4a. The presence of IBU, however, led to a small, but repeatable increase in the intensity of the water peaks. By fitting the spectra (the details for the fitting procedure are provided in the Materials and Methods section in the Supporting Information), the oscillator strengths of the 3200 and 3400 cm^{-1} peaks were both found to go up by ∼16% (Table S1). The increase in the water peaks should stem from the adsorption of the negatively charged IBU at the membrane surface, which in turn, can better align the interfacial water molecules.[33,34] Measurements were also taken with 1 and 10 μM IBU in the subphase (Figure S5). The relative increase in the oscillator strength of the 3200 cm^{-1} peak, which correlates to an increasing interfacial potential,[35,36] could be plotted as a function of bulk IBU concentration (Figure S6). This data fit well to a Langmuir isotherm. The $K_{D,app}$ value based on the VSFS measurements was 3.0 ± 1.2 μM, which is slightly weaker than the value obtained from the fluorescence assay. The phosphate group vibrational stretch of PC lipids was also examined with and without 5 μM IBU. The spectral changes were negligible in this case (Figure S7).

All of the experiments described above were performed in the presence of 50 mM phosphate buffer. As an additional test to confirm that the first binding step was dominated by electrostatics, we also ran the fluorescence measurements with 10 mM phosphate buffer, where electrostatic screening should be reduced and the interactions should presumably tighten.[37,38] The binding curve for 99.5 mol % POPC under these conditions is provided in Figure S8. In this case, the binding indeed was tightened by almost a factor of 2 (K_D = 0.48 ± 0.12 μM), in agreement with an electrostatic binding mechanism.

One source of the interaction between IBU and PC lipids should be ion pairing between the carboxylate groups of IBU and the choline groups on the PC lipids. Indeed, the adsorption of negatively charged analytes to PC lipids has been widely reported for small molecules and nanoparticles.[30,39,40] Additionally, cation−π interactions between the choline moiety on the PC headgroup and the benzene ring on the IBU may play a role.[41−43] These types of electrostatic interactions should have K_D values in the low mM range.[43,44] The apparently tighter binding in this case can be explained by a rebinding model (detailed analysis is provided in the Materials and Methods section in the Supporting Information).[45,46] In other words, upon adsorption to the lipid membrane−water interface, small molecule drugs may dissociate, diffuse laterally along the surface and rebind. As such, an apparently lower k_{off} value would contribute to the apparently tighter $K_{D,app}$ value.[47]

Step 2: Hydrophobic Insertion of IBU into PC Lipid Monolayer. As observed in Figure 3a, the second binding step between IBU and POPC bilayers essentially saturated at 300 μM. As such, Langmuir monolayer compression experiments were conducted with IBU concentrations ranging from 0 to 300 μM (Figure 5a). Again, DLPC was used in the monolayer experiments to avoid lipid oxidation. As can be seen, the DLPC isotherm gradually shifted to larger area per molecule with increasing concentrations of IBU, indicating that IBU intercalated between the PC lipids and expanded the monolayer.[48,49] Plotting the area change as a function of IBU concentration yields a binding curve for the second step with K_D = 48 ± 9 μM (Figure S9). This value is in reasonable agreement with the number obtained by fluorescence.

The interaction mechanism at this step was further explored by VSFS measurements (Figure 5b). Experiments were first conducted with DLPC monolayers. Upon introduction of 300 μM IBU into the subphase, no prominent spectral change in the CH stretch region was found. It should be noted that the slight intensity increase observed for the 2946 cm^{-1} peak was due to constructive interference with the water rather than a change in the oscillator strength (Table S2). The lack of change in the CH stretch region was because the DLPC

DOI: 10.1021/acs.langmuir.8b01878
Langmuir 2018, 34, 10782−10792

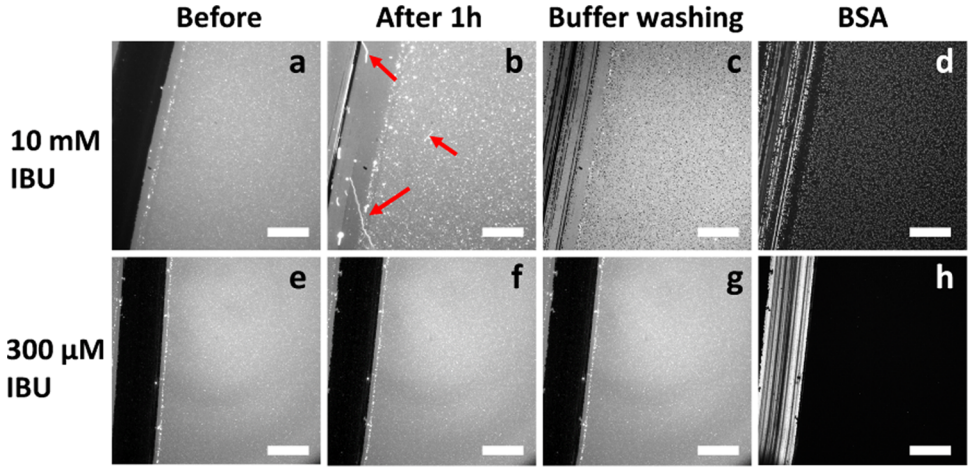

Figure 6. (a, e) Bilayers with 99.5 mol % POPC and 0.5 mol % *o*LRB−POPE before incubation with IBU; (b, f) after 1 h incubation with 10 mM IBU and 300 μM IBU, respectively; (c, g) bilayer (b) and bilayer (f) after copious rinsing with buffer; (d, h) bilayers (c) and (g) after incubation with Alexa488 labeled bovine serum albumin (BSA). Images (a)−(c) and (e)−(g) were taken with the 560 nm excitation channel, and the emission wavelength of *o*LRB was 580 nm. Images (d) and (h) were taken with the 488 nm excitation channel, and the emission wavelength of AlexaFluor-488 was 525 nm. Scale bar: 20 μm.

monolayer was already in the fluid phase to begin with. As such, the intercalation of IBU did not substantially alter the lipid tail configuration. To confirm this, analogous measurements were made with gel phase 1,2-dipalmitoyl-*sn*-glycero-3-phosphocholine (DPPC) monolayers, in which IBU showed a fluidization effect on the packing of the lipid acyl chains in this concentration range. However, similar to DLPC, when introducing only 5 μM of IBU into the subphase of the DPPC monolayer, no spectral changes in the CH stretch region were observed (Figure S11).

There was a prominent increase in the signal from the water region with DLPC (Figure 5b). The increase in oscillator strengths of the 3200 and 3400 cm^{-1} peaks were 51 and 44%, respectively (Table S2). The rise in the water peak oscillator strength with 300 μM IBU was about three times that found with 5 μM, which correlated well with the fluorescence signal change in the pH modulation assay. We conclude that the second binding step involved deeper penetration of IBU into the lipid layer. This should correlate with hydrophobic interactions with the lipid acyl chains. Indeed, IBU not only intercalated into the PC lipid monolayer and expanded the membrane area, but could also disrupt the packing of condensed phase PC lipids.

Step 3: Detergent-like Effect at mM Concentrations of IBU. The linearly increasing fluorescence signal in Figure 3b from 300 μM to 15 mM of IBU represents an unsaturable interaction with the membrane, which is an indication of three-dimensional structures forming on the lipid membrane. To study this phenomenon more directly, IBU incubation experiments were performed while monitoring the supported bilayer by epifluorescence microscopy. As can be seen, a bilayer containing 99.5 mol % POPC and 0.5 mol % *o*LRB−POPE was initially uniform (Figure 6a). The dark stripe on the left hand side of the image is a scratch made with a pair of tweezers that was used to remove a portion of the membrane from the surface to provide contrast.[50] Next, the bilayer was incubated with 10 mM IBU and imaged after 1 h (Figure 6b). Tubular structures could be seen emerging from the bilayer surface, as indicated by the red arrows. The bright spots in this image are a top view of standing tubules, which can be clearly observed under a 100× objective (Movie S1). Moreover, the scratch began to fill in with lipid material.

Next, the bilayer was washed copiously with buffer solution to rinse away any loosely attached material. Under these circumstances, dark spots were clearly evident with submicrometer diameters (Figure 6c). A histogram of the spot sizes is shown in Figure S12. The size distribution follows an exponential decay, with the largest number of the spots falling into the smallest size bin. The formation of dark spots could either be holes formed in the membrane or the formation of lipid domains, which exclude the dye.[51] To distinguish between these possibilities, protein backfilling experiments were conducted with Alexa488 labeled bovine serum albumin (BSA). PC bilayers are known to be fairly resistant to protein adsorption, but BSA can readily stick to and spread on a bare glass surface.[52,53] As such, Alexa488 labeled BSA will show up as bright spots if the initially dark spots were the result of lipid removal. As can be seen, the initially dark spots in Figure 6c became bright spots in Figure 6d (for merged images, see Figure S13). Moreover, the unfilled stripes in the scratched region were also covered with adsorbed protein. Therefore, we conclude that exposure to 10 mM IBU leads to three-dimensional structure formation as well as solubilization of the bilayer.

Similar incubation experiments were conducted with 300 μM IBU as a control. The bilayer uniformity before and after incubation appeared to be essentially unchanged in this case (Figure 6e,f). Moreover, washing the surface caused no marked changes (Figure 6g). After introduction of BSA, the Alexa488 fluorescence was only observed in the scratched region (Figure 6h). This finding confirms that at concentrations of IBU below the onset of the third step, the lipid membrane remained intact.

One curious effect of adding 10 mM IBU is the spreading of the bilayer into the scratch region as seen in Figure 6b. In this case, the attractive van der Waals interactions between the lipid bilayer and the substrate[26] along with the decreasing membrane bending modulus[11] and the membrane stretch modulus[24] due to IBU insertion acted in concert to overcome the frictional interaction between the bilayer and the substrate. As such, the bilayer was able to spread into the rougher

DOI: 10.1021/acs.langmuir.8b01878
Langmuir 2018, 34, 10782−10792

scratched regions. Another important point is that substantially more drug molecules should be located in the upper leaflet upon hydrophobic insertion than in the lower leaflet. There are two reasons for this. First, the upper leaflet is the one that is readily accessible upon initial IBU−bilayer interactions. Second, the drug should remain there because of electrostatic repulsion between IBU and the glass support, which will be much greater when the drug molecule is in the lower leaflet.[54] Such asymmetric accumulation along with the intrinsic curvature of IBU should cause tubule formation.[55]

Langmuir monolayer compression experiments were also conducted with DLPC at high concentrations of IBU, and the results support the idea of a detergent effect from IBU (Figure 7). With increasing concentrations of IBU in the mM range,

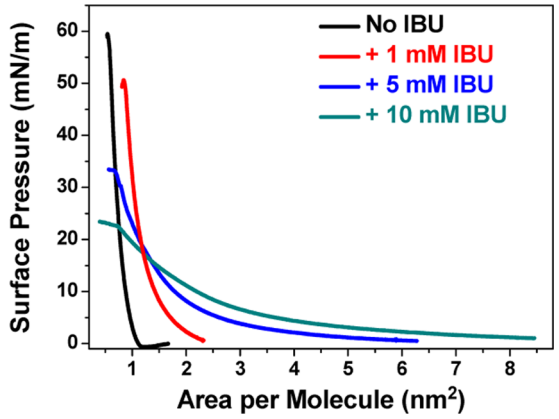

Figure 7. Surface pressure−area isotherms of DLPC monolayers before and after the introduction of 0, 1, 5 and 10 mM IBU into the aqueous subphase.

the DLPC isotherm was not further shifted to larger molecular areas compared to 300 μM IBU. Instead, the pressure at which the DLPC monolayer collapsed decreased from 58 mN/m with 0 IBU to 25 mN/m with 10 mM IBU. Also, with 5 mM IBU and above, the monolayer isotherm changed its shape to have a much shallower slope, suggesting a gradually more compressible and less stable monolayer.[14] Both changes are indicative of monolayer disruption and solubilization.[56]

Varying the Lipid Composition Alters IBU Binding. Positively charged DOTAP, negatively charged POPG, cholesterol, and zwitterionic POPE were introduced into PC-containing bilayers separately, and each of these affected the IBU binding process (Figure 8). The mole fractions of POPG, cholesterol and POPE were chosen to roughly match their average concentrations in the membranes of mammal cells.[25]

Bilayers containing 10 mol % DOTAP showed three consecutive binding steps with IBU (Figure 8a,b). The binding constants are provided in Table 1. Compared to pure POPC bilayers, the first and second steps were both tightened. The tightening of the second step could be explained in terms of an increase in the bound IBU concentration upon the saturation of the first step (Table S4), which facilitated the subsequent hydrophobic insertion. Significantly, in the membrane solubilization concentration range, bilayers with DOTAP showed a fluorescence profile that could be fit to a simple Langmuir binding isotherm. This saturable binding profile, as opposed to a linearly increasing fluorescence signal, indicated that DOTAP containing SLBs produced only a finite number of out-of-plane protrusions upon addition of mM concentrations of IBU, which acted as saturable binding sites (Movie S2 and Figure S14). This result can be attributed to both electrostatic attractions between DOTAP and the underlying negatively charged glass substrate, and a "stitching" effect by DOTAP, which has been reported to stabilize PC bilayers and may attenuate bilayer disruption.[57]

Next, incorporation of 10 mol % negatively charged POPG appeared to eliminate the first binding step (Figure 8c). This further demonstrates that the first binding step between IBU and pure PC bilayers is dominated by electrostatic interactions. Indeed, it can seemingly be removed by adding a negative charge to the membrane. As such, a separate first binding step probably does not occur on electrostatic grounds. Moreover, the second binding event between IBU and POPG-doped bilayers occurred at significantly higher IBU concentrations compared with pure POPC (Table 1). Since the signal change was about a factor of 5 smaller than in the absence of POPG, this suggests lower IBU loading at saturation. Therefore, the single binding event with K_D = 306 μM should represent a combination of electrostatic and hydrophobic insertion interactions. Moreover, the lack of an initial adsorbed layer appears to substantially weaken the K_D value for insertion compared to bilayers without PG. In the high-concentration range of IBU, bilayers with POPG displayed a linearly increasing fluorescence signal change just as with pure POPC bilayers (Figure 8d). This is in agreement with the idea that hydrophobic intercalation reached saturation, before entering the solubilization step (Movie S3 and Figure S14). The slope of the linear fit in this case was 0.036, whereas the slope of step 3 for pure POPC bilayers was 0.16, indicating that the degree of solubilization was electrostatically impeded with POPG containing bilayers and which explains the lower number of tubules in Figure S14.

Introduction of 20 mol % cholesterol into the lipid membranes yielded two binding steps for IBU (Figure 8e,f and Table 1). The first binding step was essentially unchanged from pure POPC, whereas the second one was weakened by about 2 orders of magnitude. This is consistent with the membrane condensing effect of cholesterol.[58] Indeed, cholesterol does not significantly alter interfacial electrostatic interactions. But by condensing the membrane, the cholesterol makes it harder for IBU to insert. A similar conclusion was reported with X-ray diffraction measurements.[59] Though cholesterol was expected to have a protective effect against membrane deformation and solubilization, tubules and holes were still observed on bilayers with 20 mol % cholesterol after incubation with 10 mM IBU (Movie S4). The holes and tubules, however, appeared to be less prominent (i.e., smaller and fewer in number) and apparently provided fewer binding sites compared to pure POPC bilayers (Figure S14). The number of available binding sites should increase, as IBU is added to the membrane. This led to a linear increase in fluorescence in POPC membranes. The number of sites, however, must not increase as dramatically when cholesterol is present, which resulted instead in a saturable insertion step in the mM range.

Finally, experiments were conducted with 20 mol % POPE in POPC membranes (Figure 8g,h and Table 1). In this case, the first binding step was tightened by just over a factor of 2 compared to pure POPC bilayers. This is likely the consequence of hydrogen bonding between the amine groups on the PE and the carboxylate moiety from IBU.[22] The reason why hydrogen bonding only tightened the binding by a factor

DOI: 10.1021/acs.langmuir.8b01878
Langmuir 2018, 34, 10782−10792

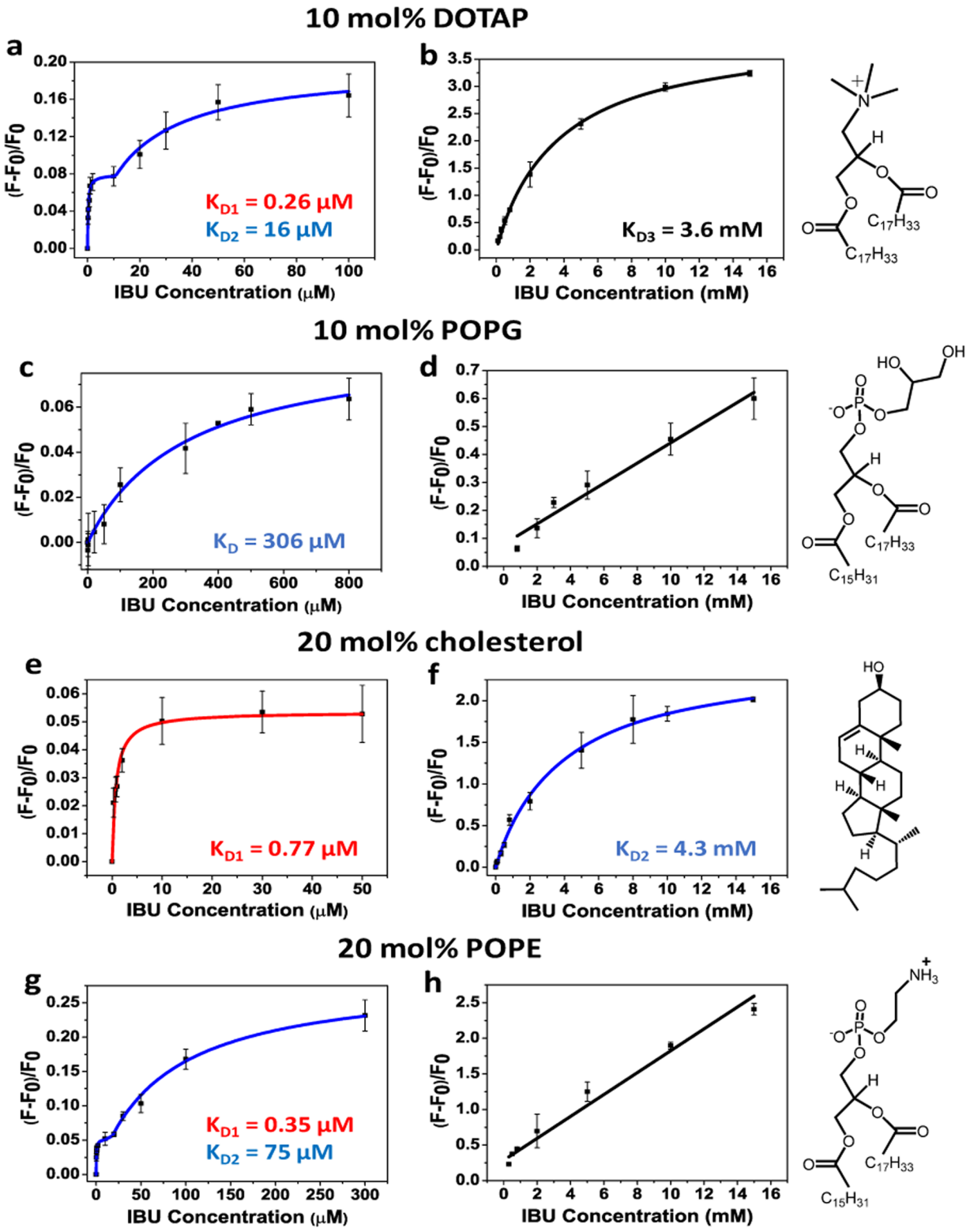

Figure 8. Binding profiles of IBU to bilayers with different lipid compositions. All the membranes contained 0.5 mol % *o*LRB−POPE: (a, b) 10 mol % DOTAP, 89.5 mol % POPC; (c, d) 10 mol % POPG, 89.5 mol % POPC; (e, f) 20 mol % cholesterol, 79.5 mol % POPC; (g, h) 20 mol % POPE, 79.5% POPC. The black dots are data points. The red curve represents the fitted results for step 1 (step 1 for (a) and (g) are displayed in Figure S15a,b, and the low concentration region for (c) is displayed in Figure S15c). The blue curves represent the fitted results for step 2 or a combination of steps 1 and 2. The black curve corresponds to the fitted result for step 3. Headgroup structures of each lipid component are shown on the right side of corresponding binding profiles. The loading differences with different membrane compositions are displayed in Table S4.

of 2 could be due to the intrinsic hydrogen bonding network between the amines on PE and the phosphate groups on both PC and PE, which competed for hydrogen bonding with IBU.[60] Interestingly, the binding at the second step was weakened. Indeed, due to the hydrogen bond-donating ability of the amine, bilayers with POPE were already more tightly

DOI: 10.1021/acs.langmuir.8b01878
Langmuir 2018, 34, 10782−10792

Table 1. Apparent Dissociation Constants ($K_{D,app}$) of IBU−Membrane Interactions with Various Membrane Compositions

	99.5 mol % POPC	89.5 mol % POPC + 10 mol % DOTAP	89.5 mol % POPC + 10 mol % POPG	79.5 mol % POPC + 20 mol % Chol	79.5 mol % POPC + 20 mol % POPE
K_{D1} (μM) electrostatic adsorption	0.88 ± 0.28	0.26 ± 0.12	NA	0.77 ± 0.30	0.35 ± 0.14
K_{D2} (μM) hydrophobic insertion	30 ± 8	16 ± 6	306 ± 100	4300 ± 1100	75 ± 20
K_{D3} (mM) membrane disruption	NA	3.6 ± 0.4	NA	NA	NA

packed compared to those made from just POPC lipids.[60] Similar phenomena have been observed when incorporating peptides into lipid membranes containing significant concentrations of POPE.[61] The third interaction step in Figure 8h showed a linearly increasing fluorescence signal change (slope = 0.15) similar to pure POPC bilayers, which correlated to membrane disruption (Movie S5 and Figure S14). Due to the intrinsic negative curvature of PE lipids, PE containing bilayers were more easily deformed than pure POPC bilayers and produced more tubules (Figure S14).[62]

DISCUSSION

Analogous to the results shown herein, multiple consecutive binding steps with lipid membranes, like those in Figures 3 and 8, have been reported for antimicrobial peptides (AMPs).[63,64] Specifically, a three-step interaction mode with lipid membranes was proposed for several types of AMPs, with the first step involving interfacial adsorption, the second step centered on hydrophobic insertion and alignment in the lipid tail region, and the third step associated with membrane disruption and hole formation.[63,64] Though IBU and AMPs have very substantial size and structural differences, it would appear that their similar binding and disruption behavior at lipid membranes can be attributed to their similar amphiphilic properties.

The first adsorption step of IBU in the lipid headgroup region should be an entropically driven process,[65,66] releasing water molecules from the hydrated negatively charged IBU.[10] Previous small angle neutron diffraction and MD simulation studies showed that when IBU was adsorbed in the lipid headgroup region, it led to membrane thinning and a decrease in the membrane bending modulus.[10,11,13] Moreover, by conducting fluorescence recovery after photobleaching experiments, we observed an increase in the diffusion constant for Texas Red-1,2-dihexadecanoyl-*sn*-glycero-3-phosphoethanolamine (DHPE) in POPC SLBs when 10 μM IBU was present (Figure S17). This indicated that the first adsorbed layer increased membrane fluidity (Figure S17), which almost certainly also decreased the area stretch modulus of the bilayer.[24] This should help facilitate hydrophobic insertion in the second binding step.

This work is the first to reveal that adsorption and insertion often represent two distinct steps, where the first facilitates the second. Nevertheless, a few other anti-inflammatory, amphiphilic small molecule drugs have been reported to show dose-dependent effects when interacting with lipid membranes. For instance, meloxicam, resveratrol, and cortisone show complex binding behavior with concentration.[67−69] At low concentrations, these drugs favor the lipid headgroup region, whereas at higher concentrations, they begin to penetrate more deeply into the lipid bilayer core region. Taken together with our studies of IBU, we hypothesize that the dose-dependent multistep binding of amphiphilic small molecules with lipid membranes may be quite common. However, the membrane disruption step at high concentration is not necessarily universal. After hydrophobic insertion, depending on the specific structure of an amphiphilic small molecule, it can either stiffen or fluidize the lipid membrane.[1,68]

On the basis of previous pharmaceutical studies, the effective concentration of IBU in the blood stream at the proper dose of the drug is between 100 and 200 μM,[70] suggesting that the most physiologically relevant concentration of IBU involves the second binding step from our results. In this case, IBU is expected to hydrophobically insert into the membranes of inflammatory cells, which are extremely fluid and unstable because of the presence of lysophospholipids and highly unsaturated tails.[71,72] As such, drug transport is expected to be remarkably efficient. COX enzymes are located in the membranes of the endoplasmic reticulum (ER) and nuclear envelope with their α-helical entrances for substrates embedded in the lipid bilayer core region.[73] IBU works as a competitive inhibitor and binds to the COX enzymes, which in turn prevents inflammation.[73] ER membranes are known for loose packing, with high concentrations of PC and PE and a relatively low concentration of cholesterol and negatively charged lipids.[25] On the basis of the current binding study (Figure 8), such a composition should favor the accumulation of IBU molecules in ER membranes.

It may be hypothesized that IBU competes with the natural substrate, arachidonic acid, for binding sites in a two-step process.[73] First, the drug would undergo hydrophobic insertion into lipid bilayers and then laterally diffuse within the membrane to the entrance sites on target proteins. Moreover, the high-concentration regime in our studies may correspond to conditions of IBU overdose. Indeed, concentrations of IBU associated with an overdose are known to cause hemorrhaging, gastrointestinal tract bleeding/ulcers, and anemia.[4] This would be consistent with conditions where the bilayer starts to solubilize. Moreover, deformation of membranes can have serious effects on the function of membrane-anchored target proteins, which may be another aspect of drug overdose.

ASSOCIATED CONTENT

Supporting Information

The Supporting Information is available free of charge on the ACS Publications website at DOI: 10.1021/acs.langmuir.8b01878.

VSFS spectra of a DLPC monolayer with 1 and 10 μM IBU, a binding curve of the first binding step based on VSFS measurements, VSFS spectra of the phosphate stretch region of DLPC with and without 5 μM IBU, a binding curve of the first step in 10 mM phosphate buffer, a binding curve of the second step based on π−A diagram measurements, a VSFS spectrum of 300 μM IBU, VSFS spectra of the DPPC CH stretch region with and without 5, 150 and 300 μM IBU, a histogram of the

DOI: 10.1021/acs.langmuir.8b01878
Langmuir 2018, 34, 10782−10792

hole sizes in POPC SLBs after incubating with 10 mM IBU, a merged fluorescence image of the holes with an image after backfilling with Alexa488 labeled proteins, tubule counts on SLBs with five different lipid compositions, binding curves of the first step between IBU and SLBs containing 10 mol % DOTAP, 20 mol % POPE and 10 mol % POPG, respectively, diffusion constants in POPC SLBs with 10 and 300 μM IBU, and tables with fitting parameters for the VSFS spectra, a table with drug loading analysis in different membrane compositions (PDF)

Tubule structures in POPC bilayers after 1 h incubation with 10 mM IBU (AVI)

Tubule structures in 10 mol % DOTAP bilayers after 1 h incubation with 10 mM IBU (AVI)

Tubule structures in 10 mol % POPG bilayers after 1 h incubation with 10 mM IBU (AVI)

Tubule structures in 20 mol % cholesterol bilayers after 1 h incubation with 10 mM IBU (AVI)

Tubule structures in 20 mol % POPE bilayers after 1 h incubation with 10 mM IBU (AVI)

AUTHOR INFORMATION

Corresponding Author

*E-mail: psc11@psu.edu.

ORCID

Paul S. Cremer: 0000-0002-8524-0438

Notes

The authors declare no competing financial interest.

ACKNOWLEDGMENTS

We acknowledge support from the Office of Naval Research (N00014-14-1-0792) and the National Science Foundation (CHE-1709735).

REFERENCES

(1) Lúcio, M.; Lima, J. L. F. C.; Reis, S. Drug-Membrane Interactions: Significance for Medicinal Chemistry. *Curr. Med. Chem.* **2010**, *17*, 1795−1809.

(2) Pande, A. H.; Qin, S.; Tatulian, S. A. Membrane Fluidity Is a Key Modulator of Membrane Binding, Insertion, and Activity of 5-Lipoxygenase. *Biophys. J.* **2005**, *88*, 4084−4094.

(3) Theumer, M. G.; Clop, E. M.; Rubinstein, H. R.; Perillo, M. A. The Lipid-Mediated Hypothesis of Fumonisin B1 Toxicodynamics Tested in Model Membranes. *Colloids Surf., B* **2008**, *64*, 22−33.

(4) Lichtenberger, L. M.; Zhou, Y.; Dial, E. J.; Raphael, R. M. NSAID Injury to the Gastrointestinal Tract: Evidence that NSAIDs Interact with Phospholipids to Weaken the Hydrophobic Surface Barrier and Induce the Formation of Unstable Pores in Membranes. *J. Pharm. Pharmacol.* **2006**, *58*, 1421−1428.

(5) Schreier, S.; Malheiros, S. V. P.; de Paula, E. Surface Active Drugs: Self-Association and Interaction with Membranes and Surfactants. Physicochemical and Biological Aspects. *Biochim. Biophys. Acta.* **2000**, *1508*, 210−234.

(6) Lichtenberger, L. M.; Zhou, Y.; Jayaraman, V.; Doyen, J. R.; O'Neil, R. G.; Dial, E. J.; Volk, D. E.; Gorenstein, D. G.; Boggara, M. B.; Krishnamoorti, R. Insight into NSAID-Induced Membrane Alterations, Pathogenesis and Therapeutics: Characterization of Interaction of NSAIDs with Phosphatidylcholine. *Biochim. Biophys. Acta.* **2012**, *1821*, 994−1002.

(7) Zapolska-Downar, D.; Zapolski-Downar, A.; Bukowska, H.; Galka, H.; Naruszewicz, M. Ibuprofen Protects Low Density Lipoproteins Against Oxidative Modification. *Life Sci.* **1999**, *65*, 2289−2303.

(8) Morihara, T.; Teter, B.; Yang, F.; Lim, G. P.; Boudinot, S.; Boudinot, F. D.; Frautschy, S. A.; Cole, G. M. Ibuprofen Suppresses Interleukin-1β Induction of Pro-Amyloidogenic α1-Antichymotrypsin to Ameliorate β-Amyloid (Aβ) Pathology in Alzheimer's Models. *Neuropsychopharmacology* **2005**, *30*, 1111−1120.

(9) Harris, R. E.; Beebe-Donk, J.; Doss, H.; Burr Doss, D. Aspirin, Ibuprofen, and Other Non-Steroidal Anti-Inflammatory Drugs in Cancer Prevention: A Critical Review of Non-Selective COX-2 Blockade. *Oncol. Rep.* **2005**, *13*, 559−583.

(10) Boggara, M. B.; Mihailescu, M.; Krishnamoorti, R. Structural Association of Nonsteroidal Anti-Inflammatory Drugs with Lipid Membranes. *J. Am. Chem. Soc.* **2012**, *134*, 19669−19676.

(11) Boggara, M. B.; Faraone, A.; Krishnamoorti, R. Effect of pH and Ibuprofen on the Phospholipid Bilayer Bending Modulus. *J. Phys. Chem. B* **2010**, *114*, 8061−8066.

(12) Fox, C. B.; Horton, R. A.; Harris, J. M. Detection of Drug−Membrane Interactions in Individual Phospholipid Vesicles by Confocal Raman Microscopy. *Anal. Chem.* **2006**, *78*, 4918−4924.

(13) Boggara, M. B.; Krishnamoorti, R. Partitioning of Nonsteroidal Anti-inflammatory Drugs in Lipid Membranes: A Molecular Dynamics Simulation Study. *Biophys. J.* **2010**, *98*, 586−595.

(14) Jabłonowska, E.; Bilewicz, R. Interactions of Ibuprofen with Langmuir Monolayers of Membrane Lipids. *Thin Solid Films* **2007**, *515*, 3962−3966.

(15) Du, L.; Liu, X.; Huang, W.; Wang, E. A Study on the Interaction between Ibuprofen and Bilayer Lipid Membrane. *Electrochim. Acta* **2006**, *51*, 5754−5760.

(16) Manrique-Moreno, M.; Heinbockel, L.; Suwalsky, M.; Garidel, P.; Brandenburg, K. Biophysical Study of the Non-Steroidal Anti-Inflammatory Drugs (NSAID) Ibuprofen, Naproxen and Diclofenac with Phosphatidylserine Bilayer Membranes. *Biochim. Biophys. Acta* **2016**, *1858*, 2123−2131.

(17) Jaksch, S.; Lipfert, F.; Koutsioubas, A.; Mattauch, S.; Holderer, O.; Ivanova, O.; Frielinghaus, H.; Hertrich, S.; Fischer, S.; Nickel, B. Influence of Ibuprofen on Phospholipid Membranes. *Phys. Rev. E* **2015**, *91*, No. 022716.

(18) Geraldo, V. P. N.; Pavinatto, F. J.; Nobre, T. M.; Caseli, L.; Oliveira, O. N., Jr. Langmuir Films Containing Ibuprofen and Phospholipids. *Chem. Phys. Lett.* **2013**, *559*, 99−106.

(19) Jung, H.; Robison, A. D.; Cremer, P. S. Detecting Protein−Ligand Binding on Supported Bilayers by Local pH Modulation. *J. Am. Chem. Soc.* **2009**, *131*, 1006−1014.

(20) Huang, D.; Robison, A. D.; Liu, Y.; Cremer, P. S. Monitoring Protein−Small Molecule Interactions by Local pH Modulation. *Biosens. Bioelectron.* **2012**, *38*, 74−78.

(21) Robison, A. D.; Huang, D.; Jung, H.; Cremer, P. S. Fluorescence Modulation Sensing of Positively and Negatively Charged Proteins on Lipid Bilayers. *Biointerphases* **2013**, *8*, 1−9.

(22) Huang, D.; Zhao, T.; Xu, W.; Yang, T.; Cremer, P. S. Sensing Small Molecule Interactions with Lipid Membranes by Local pH Modulation. *Anal. Chem.* **2013**, *85*, 10240−10248.

(23) Robison, A. D.; Sun, S.; Poyton, M. F.; Johnson, G. A.; Pellois, J.; Jungwirth, P.; Vazdar, M.; Cremer, P. S. Polyarginine Interacts More Strongly and Cooperatively than Polylysine with Phospholipid Bilayers. *J. Phys. Chem. B* **2016**, *120*, 9287−9296.

(24) Picas, L.; Rico, F.; Scheuring, S. Direct Measurement of the Mechanical Properties of Lipid Phases in Supported Bilayers. *Biophys. J.* **2012**, *102*, L01−L03.

(25) van Meer, G.; Voelker, D. R.; Feigenson, G. W. Membrane Lipids: Where They Are and How They Behave. *Nat. Rev. Mol. Cell Biol.* **2008**, *9*, 112−124.

(26) Cremer, P. S.; Boxer, S. G. Formation and Spreading of Lipid Bilayers on Planar Glass Supports. *J. Phys. Chem. B* **1999**, *103*, 2554−2559.

(27) Nguyen, T. T.; Rembert, K.; Conboy, J. C. Label-Free Detection of Drug-Membrane Association Using Ultraviolet−Visible Sum-Frequency Generation. *J. Am. Chem. Soc.* **2009**, *131*, 1401−1403.

(28) Mangiarotti, A.; Caruso, B.; Wilke, N. Phase Coexistence in Films Composed of DLPC and DPPC: A Comparison between

DOI: 10.1021/acs.langmuir.8b01878
Langmuir 2018, 34, 10782−10792

Different Model Membrane Systems. *Biochim. Biophys. Acta* **2014**, *1838*, 1823−1831.
(29) Alhakamy, N. A.; Kaviratna, A.; Berkland, C. J.; Dhar, P. Dynamic Measurements of Membrane Insertion Potential of Synthetic Cell Penetrating Peptides. *Langmuir* **2013**, *29*, 15336−15349.
(30) Okuno, M.; Mezger, M.; Stangenberg, R.; Baumgarten, M.; Müllen, K.; Bonn, M.; Backus, E. H. G. Interaction of a Patterned Amphiphilic Polyphenylene Dendrimer with a Lipid Monolayer: Electrostatic Interactions Dominate. *Langmuir* **2015**, *31*, 1980−1987.
(31) Sovago, M.; Wurpel, G. W. H.; Smits, M.; Müller, M.; Bonn, M. Calcium-Induced Phospholipid Ordering Depends on Surface Pressure. *J. Am. Chem. Soc.* **2007**, *129*, 11079−11084.
(32) Mondal, J. A.; Nihonyanagi, S.; Yamaguchi, S.; Tahara, T. Three Distinct Water Structures at a Zwitterionic Lipid/Water Interface Revealed by Heterodyne-Detected Vibrational Sum Frequency Generation. *J. Am. Chem. Soc.* **2012**, *134*, 7842−7850.
(33) Wu, F.; Yang, P.; Zhang, C.; Han, X.; Song, M.; Chen, Z. Investigation of Drug−Model Cell Membrane Interactions Using Sum Frequency Generation Vibrational Spectroscopy: A Case Study of Chlorpromazine. *J. Phys. Chem. C* **2014**, *118*, 17538−17548.
(34) Wu, F.-G.; Yang, P.; Zhang, C.; Li, B.; Han, X.; Song, M.; Chen, Z. Molecular Interactions between Amantadine and Model Cell Membranes. *Langmuir* **2014**, *30*, 8491−8499.
(35) Gurau, M. C.; Kim, G.; Lim, S. M.; Albertorio, F.; Fleisher, H. C.; Cremer, P. S. Organization of Water Layers at Hydrophilic Interfaces. *ChemPhysChem* **2003**, *4*, 1231−1233.
(36) Jena, K. C.; Hore, D. K. Variation of Ionic Strength Reveals the Interfacial Water Structure at a Charged Mineral Surface. *J. Phys. Chem. C* **2009**, *113*, 15364−15372.
(37) Newton, A. C. Interaction of Proteins with Lipid Headgroups: Lessons from Protein Kinase C. *Annu. Rev. Biophys. Biomol. Struct.* **1993**, *22*, 1−25.
(38) Li, S.; Malmstadt, N. Deformation and Poration of Lipid Bilayer Membranes by Cationic Nanoparticles. *Soft Matter* **2013**, *9*, 4969−4976.
(39) Michanek, A.; Kristen, N.; Höök, F.; Nylander, T.; Sparr, E. RNA and DNA Interactions with Zwitterionic and Charged Lipid Membranes—A DSC and QCM-D Study. *Biochim. Biophys. Acta* **2010**, *1798*, 829−838.
(40) Wang, B.; Zhang, L.; Bae, S. C.; Granick, S. Nanoparticle-Induced Surface Reconstruction of Phospholipid Membranes. *Proc. Natl. Acad. Sci. U.S.A.* **2008**, *105*, 18171−18175.
(41) Grauffel, C.; Yang, B.; He, T.; Roberts, M. F.; Gershenson, A.; Reuter, N. Cation−π Interactions as Lipid-Specific Anchors for Phosphatidylinositol-Specific Phospholipase C. *J. Am. Chem. Soc.* **2013**, *135*, 5740−5750.
(42) Kearney, P. C.; Mizoue, L. S.; Kumpf, R. A.; Forman, J. E.; McCurdy, A.; Dougherty, D. A. Molecular Recognition in Aqueous Media. New Binding Studies Provide Further Insights into the Cation-Pi Interaction and Related Phenomena. *J. Am. Chem. Soc.* **1993**, *115*, 9907−9919.
(43) Gallivan, J. P.; Dougherty, D. A. A Computational Study of Cation−π Interactions vs Salt Bridges in Aqueous Media: Implications for Protein Engineering. *J. Am. Chem. Soc.* **2000**, *122*, 870−874.
(44) Kherb, J.; Flores, S. C.; Cremer, P. S. Role of Carboxylate Side Chains in the Cation Hofmeister Series. *J. Phys. Chem. B* **2012**, *116*, 7389−7397.
(45) Scheidt, H. A.; Pampel, A.; Nissler, L.; Gebhardt, R.; Huster, D. Investigation of the Membrane Localization and Distribution of Flavonoids by High-Resolution Magic Angle Spinning NMR Spectroscopy. *Biochim. Biophys. Acta* **2004**, *1663*, 97−107.
(46) Lagerholm, B. C.; Thompson, N. L. Theory for Ligand Rebinding at Cell Membrane Surfaces. *Biophys. J.* **1998**, *74*, 1215−1228.
(47) Shinohara, Y.; Hasegawa, Y.; Kaku, H.; Shibuya, N. Elucidation of the Mechanism Enhancing the Avidity of Lectin with Oligosaccharides on the Solid Phase Surface. *Glycobiology* **1997**, *7*, 1201−1208.
(48) Ege, C.; Lee, K. Y. C. Insertion of Alzheimer's Aβ40 Peptide into Lipid Monolayers. *Biophys. J.* **2004**, *87*, 1732−1740.
(49) Nunes, C.; Brezesinski, G.; Pereira-Leite, C.; Lima, J. L. F. C.; Reis, S.; Lúcio, M. NSAIDs Interactions with Membranes: A Biophysical Approach. *Langmuir* **2011**, *27*, 10847−10858.
(50) Poyton, M. F.; Sendecki, A. M.; Cong, X.; Cremer, P. S. Cu^{2+} Binds to Phosphatidylethanolamine and Increases Oxidation in Lipid Membranes. *J. Am. Chem. Soc.* **2016**, *138*, 1584−1590.
(51) Baumgart, T.; Hunt, G.; Farkas, E. R.; Webb, W. W.; Feigenson, G. W. Fluorescence Probe Partitioning between Lo/Ld Phases in Lipid Membranes. *Biochim. Biophys. Acta* **2007**, *1768*, 2182−2194.
(52) Glasmästar, K.; Larsson, C.; Höök, F.; Kasemo, B. Protein Adsorption on Supported Phospholipid Bilayers. *J. Colloid Interface Sci.* **2002**, *246*, 40−47.
(53) Wertz, C. F.; Santore, M. M. Effect of Surface Hydrophobicity on Adsorption and Relaxation Kinetics of Albumin and Fibrinogen: Single-Species and Competitive Behavior. *Langmuir* **2001**, *17*, 3006−3016.
(54) Shreve, A. P.; Howland, M. C.; Sapuri-Butti, A. R.; Allen, T. W.; Parikh, A. N. Evidence for Leaflet-Dependent Redistribution of Charged Molecules in Fluid Supported Phospholipid Bilayers. *Langmuir* **2008**, *24*, 13250−13253.
(55) Lichtenberg, D.; Ahyayauch, H.; Goñi, F. M. The Mechanism of Detergent Solubilization of Lipid Bilayers. *Biophys. J.* **2013**, *105*, 289−299.
(56) Lee, K. Y. C. Collapse Mechanisms of Langmuir Monolayers. *Annu. Rev. Phys. Chem.* **2008**, *59*, 771−791.
(57) Zhang, L.; Spurlin, T. A.; Gewirth, A. A.; Granick, S. Electrostatic Stitching in Gel-Phase Supported Phospholipid Bilayers. *J. Phys. Chem. B* **2006**, *110*, 33−35.
(58) Marquardt, D.; Kučerka, N.; Wassall, S. R.; Harroun, T. A.; Katsaras, J. Cholesterol's Location in Lipid Bilayers. *Chem. Phys. Lipids* **2016**, *199*, 17−25.
(59) Alsop, R. J.; Armstrong, C. L.; Maqbool, A.; Toppozini, L.; Dies, H.; Rheinstädter, M. C. Cholesterol Expels Ibuprofen from the Hydrophobic Membrane Core and Stabilizes Lamellar Phases in Lipid Membranes Containing Ibuprofen. *Soft Matter* **2015**, *11*, 4756−4767.
(60) Bouchet, A. M.; Frías, M. A.; Lairion, F.; Martini, F.; Almaleck, H.; Gordillo, G.; Disalvo, E. A. Structural and Dynamical Surface Properties of Phosphatidylethanolamine Containing Membranes. *Biochim. Biophys. Acta* **2009**, *1788*, 918−925.
(61) Lewis, J. R.; Cafiso, D. S. Correlation between the Free Energy of a Channel-Forming Voltage-Gated Peptide and the Spontaneous Curvature of Bilayer Lipids. *Biochemistry* **1999**, *38*, 5932−5938.
(62) Sendecki, A. M.; Poyton, M. F.; Baxter, A. J.; Yang, T.; Cremer, P. S. Supported Lipid Bilayers with Phosphatidylethanolamine as the Major Component. *Langmuir* **2017**, *33*, 13423−13429.
(63) Last, N. B.; Miranker, A. D. Common Mechanism Unites Membrane Poration by Amyloid and Antimicrobial Peptides. *Proc. Natl. Acad. Sci. U.S.A.* **2013**, *110*, 6382−6387.
(64) Huang, H. W. Action of Antimicrobial Peptides: Two-State Model. *Biochemistry* **2000**, *39*, 8347−8352.
(65) Manrique-Moreno, M.; Garidel, P.; Suwalsky, M.; Howe, J.; Brandenburg, K. The Membrane-Activity of Ibuprofen, Diclofenac, and Naproxen: A Physico-Chemical Study with Lecithin Phospholipids. *Biochim. Biophys. Acta* **2009**, *1788*, 1296−1303.
(66) Manrique-Moreno, M.; Howe, J.; Suwalsky, M.; Garidel, P.; Brandenburg, K. Physicochemical Interaction Study of Non-Steroidal Anti-Inflammatory Drugs with Dimyristoylphosphatidylethanolamine Liposomes. *Lett. Drug Des. Discovery* **2010**, *7*, 50−56.
(67) Nunes, C.; Brezesinski, G.; Lima, J. L. F. C.; Reis, S.; Lúcio, M. Synchrotron SAXS and WAXS Study of the Interactions of NSAIDs with Lipid Membranes. *J. Phys. Chem. B* **2011**, *115*, 8024−8032.
(68) Selvaraj, S.; Mohan, A.; Narayanan, S.; Sethuraman, S.; Krishnan, U. M. Dose-Dependent Interaction of *trans*-Resveratrol

DOI: 10.1021/acs.langmuir.8b01878
Langmuir 2018, 34, 10782−10792

with Biomembranes: Effects on Antioxidant Property. *J. Med. Chem.* **2013**, *56*, 970−981.
(69) Alsop, R. J.; Khondker, A.; Hub, J. S.; Rheinstädter, M. C. The Lipid Bilayer Provides a Site for Cortisone Crystallization at High Cortisone Concentrations. *Sci. Rep.* **2016**, *6*, No. 22425.
(70) Dewland, P. M.; Reader, S.; Berry, P. Bioavailability of Ibuprofen Following Oral Administration of Standard Ibuprofen, Sodium Ibuprofen or Ibuprofen Acid Incorporating Poloxamer in Healthy Volunteers. *BMC Clin. Pharmacol.* **2009**, *9*, 19.
(71) Dinkla, S.; van Eijk, L. T.; Fuchs, B.; Schiller, J.; Joosten, I.; Brock, R.; Pickkers, P.; Bosman, G. J. C. G. M. Inflammation-Associated Changes in Lipid Composition and the Organization of the Erythrocyte Membrane. *BBA Clin.* **2016**, *5*, 186−192.
(72) Calder, P. C. Long-Chain Fatty Acids and Inflammation. *Proc. Nutr. Soc.* **2012**, *71*, 284−289.
(73) Blobaum, A. L.; Marnett, L. J. Structural and Functional Basis of Cyclooxygenase Inhibition. *J. Med. Chem.* **2007**, *50*, 1425−1441.

DOI: 10.1021/acs.langmuir.8b01878
Langmuir 2018, 34, 10782−10792